CountFormer: A Transformer Framework for Learning Visual Repetition and Structure in Class-Agnostic Object Counting

1st Md Tanvir Hossain *University of Rajshahi* Rajshahi, Bangladesh mth_cse@ru.ac.bd 2nd Akif Islam *University of Rajshahi* Rajshahi, Bangladesh s1910776135@ru.ac.bd

3rd Mohd Ruhul Ameen *Marshall University* West Virginia, USA ameen@marshall.edu

Abstract-Humans can effortlessly count diverse objects by perceiving visual repetition and structural relationships rather than relying on class identity. However, most existing counting models fail to replicate this ability—they often miscount when objects exhibit complex shapes, internal symmetry, or overlapping components. In this work, we introduce CountFormer, a transformer-based framework that learns to recognize repetition and structural coherence for class-agnostic object counting. Built upon the CounTR architecture, our model replaces its visual encoder with the self-supervised foundation model DI-NOv2, which produces richer and spatially consistent feature representations. We further incorporate positional embedding fusion to preserve geometric relationships before decoding these features into density maps through a lightweight convolutional decoder. Evaluated on the FSC-147 dataset, our model achieves performance comparable to current state-of-the-art methods while demonstrating superior accuracy on structurally intricate or densely packed scenes. Our findings indicate that integrating foundation models such as DINOv2 enables counting systems to approach human-like structural perception-advancing toward a truly general and exemplar-free counting paradigm.

Index Terms—Object counting, zero-shot, DINOv2, positional embeddings, FSC-147

I. INTRODUCTION

We often pause to admire how effortlessly we count things around us as our eyes pick up repeating shapes and patterns—even if we have no idea what class they belong to. Yet when we hand this task over to a machine, the magic fades. Modern computer-vision systems shine when they are trained to count a specific class of objects: people [1], vehicles [2], or other familiar categories. But when they face objects of a completely new type, without any exemplar or prompt, they struggle. Imagine a model staring at a pair of sunglasses and, without a sense of structure, counting each lens as two separate objects. This kind of error reveals a deeper issue: the machine can see shapes, but it cannot always grasp how the parts come together.

Earlier work tried to remedy this by matching patches within an image and counting through similarity [3]. More recent efforts built on transformers to scan entire scenes and generalize to unseen classes [4]. Some vision-language systems even substitute exemplars with text prompts [5]. But

these approaches often focus on what the object is rather than how its parts are arranged, and they falter when structural coherence matters.

In our work we embrace that challenge. We introduce CountFormer, a class-agnostic counting framework designed to give machines a sense of structure. We replace the original image encoder in previous models with the self-supervised vision foundation model DINOv2 [6], which produces richer and more coherent embeddings of the scene's geometry. We then fuse two-dimensional positional embeddings into these features so the network retains geometric relationships. Finally, a lightweight convolutional decoder transforms these spatially aware features into a continuous density map whose integral yields the object count. In this way we aim to reduce structural miscounts—like the sunglasses example—while avoiding reliance on exemplars, text prompts, or heavy test-time tricks. Our contributions are:

- 1) We present CountFormer, an exemplar-free, classagnostic counting model that integrates a DINOv2 encoder to improve spatial and semantic fidelity.
- We propose positional embedding fusion, a simple yet effective way to preserve geometric relationships and lift density map accuracy in structurally ambiguous scenes.
- 3) We demonstrate via experiments on the standard FSC-147 benchmark [7] that our model delivers competitive zero-shot performance with clearer qualitative gains on composite and densely repetitive objects.
- 4) We offer an in-depth analysis of failure modes such as tightly packed objects or indistinct boundaries and draw insights to guide future development of class-agnostic counting systems.

II. RELATED WORK

A. Class-Specific Object Counting

Early works in object counting mainly targeted *class-specific* scenarios, such as crowd counting [1] or vehicle counting [2]. These approaches generally fall into two main categories: *detection-based* methods, which identify individual instances through bounding boxes, and *regression-based*

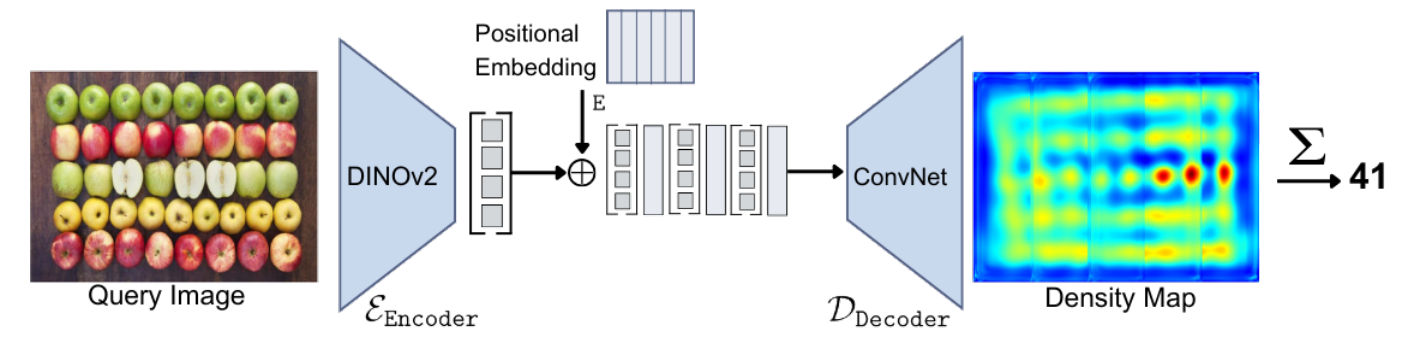


Fig. 1. Detailed overview of the proposed model architecture: Our approach utilizes a self-supervised visual encoder, specifically DINOv2, to process the query image. The extracted image features are then summed with the positional embeddings which serve as query vectors. Subsequently, we use a CNN-based decoder to decode these vectors and upscale them to generate the corresponding density map. Finally, the total object count is determined by integrating the values across the density map.

methods, which estimate object density maps whose summed pixel values yield the total count [8]. While highly effective for their target domains, these approaches lack generalization and fail when applied to unseen object types. In contrast, humans can effortlessly count diverse objects regardless of category—highlighting a gap between task-specific models and human-like perceptual flexibility.

B. Class-Agnostic and Exemplar-Free Counting

To overcome this limitation, *class-agnostic* counting methods have emerged, aiming to generalize across categories without retraining. The General Matching Network (GMN) [3] and Few-shot Adaptation and Matching Network (FamNet) [7] formulated counting as a visual matching problem—estimating similarity between patches within an image or between query and exemplar regions. However, these approaches still depend on exemplar patches provided by humans, which limits their scalability and automation.

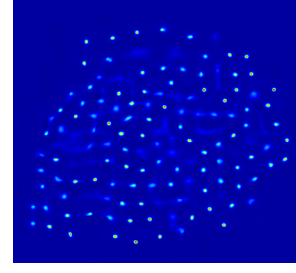
More recent research has moved toward *exemplar-free* counting. RepRPN [9] removed the need for exemplars but primarily detected the dominant object class in an image. Vision-language models (VLMs) such as CLIP-Count [5] and CounTX [10] replaced exemplars with textual prompts, leveraging CLIP [11] to align image and text features through cross-attention. While these methods reduced manual supervision, they remained dependent on well-crafted prompts, which introduces linguistic bias and limits fully automatic operation.

C. Representation Learning in Counting

Beyond architecture design, representation learning plays a crucial role in counting performance. CLIP-based methods offer rich semantic understanding but often overlook spatial structure and quantitative relationships—essential for accurate counting. Paiss et al. [12], [13] demonstrated that CLIP tends to emphasize object identity words in captions while ignoring numerical cues, leading to systematic over- or undercounting. This limitation makes CLIP-based models prone to errors in structurally complex objects, such as mistaking both lenses of a pair of glasses as two separate instances.

Attention-based and self-supervised encoders have shown promise in mitigating these issues. CounTR [4] introduced





(a) Input image (GT = 149 objects)

(b) Predicted density map (Count = 149)

Fig. 2. For the given image (left) with a ground truth of 149 objects, our model produced a density map (right) that was summed to predict an object count of 149.

a transformer-based framework that leveraged patch-level attention and positional encoding to model global context, achieving competitive zero-shot results. RCC [14] advanced this direction by incorporating a self-supervised DINO-based teacher-student framework for density regression. While effective, these encoders still struggled to capture *structural coherence*—the spatial relationships binding multiple parts into a single object.

D. DINOv2 and Structural Awareness

The recent rise of foundation models such as DINOv2 [6] has transformed self-supervised visual learning. Unlike CLIP, which learns from paired image—text data, DINOv2 learns directly from visual information, enabling it to encode both semantic meaning and spatial structure without manual labels. This allows DINOv2 to produce feature embeddings that are *structurally aware*—capturing fine-grained relationships between object parts and their spatial organization. Such representations are particularly valuable for counting tasks, where recognizing the boundaries and repetition patterns of objects is essential.

In this work, we leverage DINOv2 as a self-supervised image encoder and fuse its representations with positional embeddings to maintain geometric consistency. By doing so, we bridge the gap between semantic abstraction and spatial

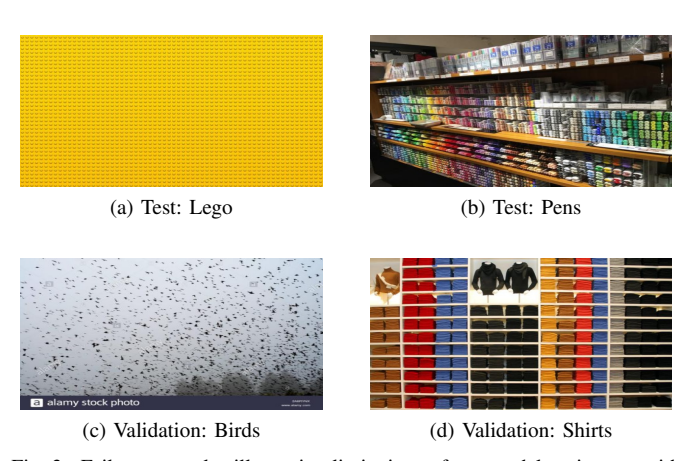


Fig. 3. Failure examples illustrating limitations of our model on images with large object counts and weak inter-object separation. Top row: test set; bottom row: validation set.

precision, enabling more reliable and interpretable zero-shot object counting—especially for complex or composite objects.

E. Research Gap and Motivation

Despite steady progress, current class-agnostic counting methods face a persistent limitation: they lack structural awareness. Models such as CounTR [4] and RCC [14] capture global attention or semantic similarity but fail to encode how object parts relate spatially within the image. As a result, they often misinterpret composite or repetitive structures—counting object fragments rather than whole instances. Existing visionlanguage models like CLIP [11] further amplify this issue by prioritizing semantics over geometry. To bridge this gap, our work introduces a structure-aware zero-shot counting framework built upon DINOv2 [6], a self-supervised foundation model that inherently preserves spatial coherence. By combining DINOv2's rich visual embeddings with positional embedding fusion and a convolutional decoder, we aim to enable more accurate counting of complex, multi-part objects without the need for exemplars or textual guidance.

III. METHODOLOGY

In this paper, we address the challenging problem of visual object counting without reference images or arbitrary exemplars provided by the users. Our objective is to train a generalized visual object counter capable of performing effectively on a test set without any exemplars. The training dataset is defined as follows:

$$D_{train} = (X_1, y_1), ..., (X_N, y_N)$$
 (1)

where $X_i \in R^{H \times W \times 3}$ represents the input image, and $y_i \in R^{H \times W \times 1}$ is a binary spatial density map. This map features 1's at the central location of the objects, denoting their presence, and 0's elsewhere where objects are absent. The total object count can be ascertained by performing a spatial summation over the density map. We aim to develop a visual object counter with a generalized approach, designed

TABLE I
COMPARISON OF ZERO-SHOT METHODS ON THE FSC-147 DATASET.
COUNTX WAS NOT ZERO-SHOT; IT USED OBJECT CLASS NAMES SPECIFIED
VIA TEXT PROMPTS.

Method	Valida	tion Set	Test Set		
	MAE	RMSE	MAE	RMSE	
GMN [3]	39.02	106.06	37.86	141.39	
FamNet [7]	32.15	98.75	32.37	131.46	
CounTX* [10]	17.70	63.61	15.73	106.88	
CounTR [4]	18.07	71.84	14.71	106.87	
RCC [14]	17.49	58.81	17.12	104.53	
Ours	19.11	65.58	19.06	118.45	

to work on a test set, even when provided with no exemplars, denoted as follows:

$$D_{test} = (X_{N+1}), ..., (X_M)$$
 (2)

We employ the DINOv2 [6] vision foundation model to execute self-supervised knowledge distillation, enhancing the model's ability to understand the feature space within the images. To preserve the spatial relationships inherent within the input images, we incorporate positional embeddings into the visual feature representations. The feature vectors, which now embody both the distilled knowledge and spatial context, are subsequently processed through a ConvNet-based decoder. This transformation yields a density map that is subsequently refined by a linear regression layer, resulting in a single-channel heatmap.

A. Dataset & Metrics

The FSC-147 [7] dataset is widely used in class-agnostic counting, and contains 6135 images across 147 object classes. The number of objects per image ranges from 7 to 3731, and averages at 56. FSC-147 provides a corresponding binary density map y_i for each training image X_i in D_{train} .

We use the standard Mean Absolute Error (MAE) and Root Mean Squared Error (RMSE) to evaluate the performance of the model.

$$MAE = \frac{1}{N} \sum_{i=1}^{N} |C_i - C_i^{GT}|,$$
 (3)

$$RMSE = \sqrt{\frac{1}{N} \sum_{i=1}^{N} (C_i - C_i^{GT})^2}$$
 (4)

Here, N refers to the number of images in the test set while C_i and C_i^{GT} refer to the predicted count and ground truth of the i-th image. The count C_i is obtained from summing the values across the density map y_i .

B. Architecture

In this section, we outline the architecture of our proposed model, which can be viewed in Figure 1. We use the DINOv2 visual encoder, denoted as $\mathcal{E}_{\texttt{Encoder}}$, that converts the input image \mathcal{X}_i into a feature map, $\mathcal{F}_{\texttt{DINO}}$. To this feature map, positional embeddings, denoted as E, are applied, yielding a spatial feature representation $\mathcal{F}_{\texttt{E}}$. A ConvNet-based decoder $\mathcal{D}_{\texttt{Decoder}}$, consist of four upsampling stages decode $\mathcal{F}_{\texttt{E}}$ into

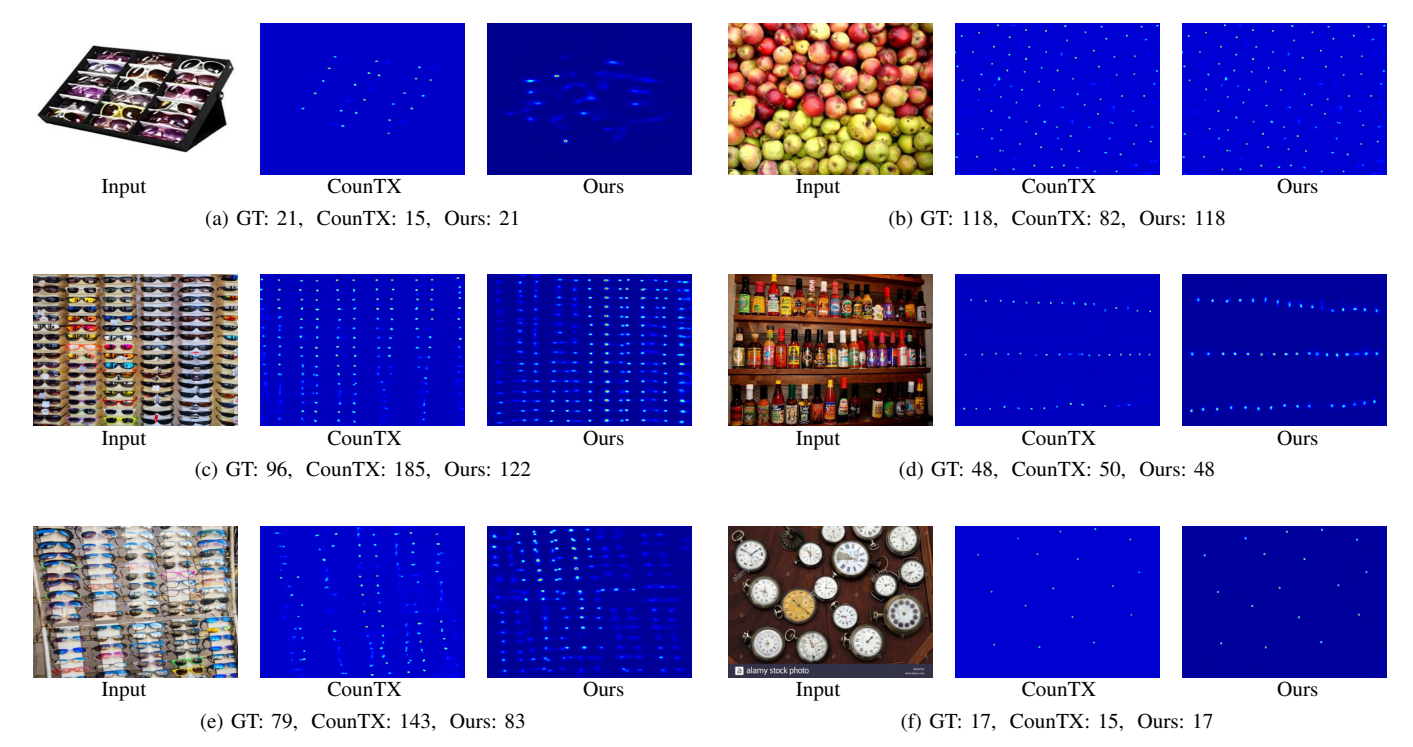


Fig. 4. Qualitative results of our model on FSC-147. Each sub-figure consists of the original image (left), CounTX's density map (middle), and our model's density map (right). The predicted counts from both models and ground truth (GT) counts have also been provided.

one-channel heatmap y_i with the original image size that signifies the density of objects within the image. The overall computational sequence is represented in Equation 5.

$$y_i = \mathcal{D}_{\mathtt{Decoder}}(\mathtt{E} + (\mathcal{E}_{\mathtt{Encoder}}(\mathcal{X}_i)))$$
 (5)

1) Visual Encoder: To learn a comprehensive and informative feature space without relying on labels, we employ a self-supervised knowledge distillation model as outlined in [6]. The concept of knowledge distillation, introduced in [15], involves training a student network, denoted as g_{θ_s} , to mimic the output of a specified teacher network g_{θ_t} . Both networks are characterized by their respective parameters, θ_s and θ_t . Given an input image x, both networks yield probability distributions across K dimensions, represented by P_s for the student and P_t for the teacher. The probability P is derived by applying the softmax function to the output of the network g. In [16], this process specify as follows,

$$P_s(x)^{(i)} = \frac{\exp(g_{\theta_s}(x)^{(i)}/\tau_s)}{\sum_{k=1}^K \exp(g_{\theta_s}(x)^{(k)}/\tau_s)}$$
(6)

with $\tau_s>0$ that controls the sharpness of the output distribution. According to [16], with a predetermined teacher network g_{θ_t} , we aim to align the distributions by minimizing the crossentropy loss between P_t and P_s , detailed as follows.

$$\min_{\theta_s} \sum_{x \in \{x_1^g, x_2^g\}} \sum_{\substack{x' \in V \\ x' \neq x}} H(P_t(x), P_s(x')) \tag{7}$$

where $H(a,b) = -a \log b$. More precisely, from a provided image, we produce a set of V comprising various views. This set includes two global views x_1^g and x_2^g , along with multiple local views at a reduced resolution. This configuration is termed the foundational parametrization of DINO. In our approach, for an input image represented by \mathcal{X}_i , our method generates a feature map $\mathcal{F}_{\text{DINO}}$ as described in Equation 8 below.

$$\mathcal{F}_{\texttt{DINO}} = \mathcal{E}_{\texttt{Encoder}}(\mathcal{X}_i) \in \mathbb{R}^{M \times D}$$
 (8)

This feature map is the result of encoding process $\mathcal{E}_{\text{Encoder}}$, transforming the input image into $M \times D$ dimensions.

2) Positional Embedding: The model needs to understand where each token comes from in the original image. We use positional embeddings E to help maintain the spatial relationships that were present in the original 2D image. The spatial structure of the image is encoded in these embeddings and is used by the model to understand the relative or absolute positions of the tokens before feeding them into the upsampling CNN layers. We add this positional embedding to the visual features to produce spatial feature representation \mathcal{F}_{E} , represented as follows.

$$\mathcal{F}_{E} = E + \mathcal{F}_{DINO} \tag{9}$$

The positional embeddings E can provide an initial encoding of spatial features that can be further processed by convolutional layers. While CNNs can extract and leverage spatial hierarchies due to their nature, the positional embeddings can provide a starting point that encodes absolute or relative positions within the image.

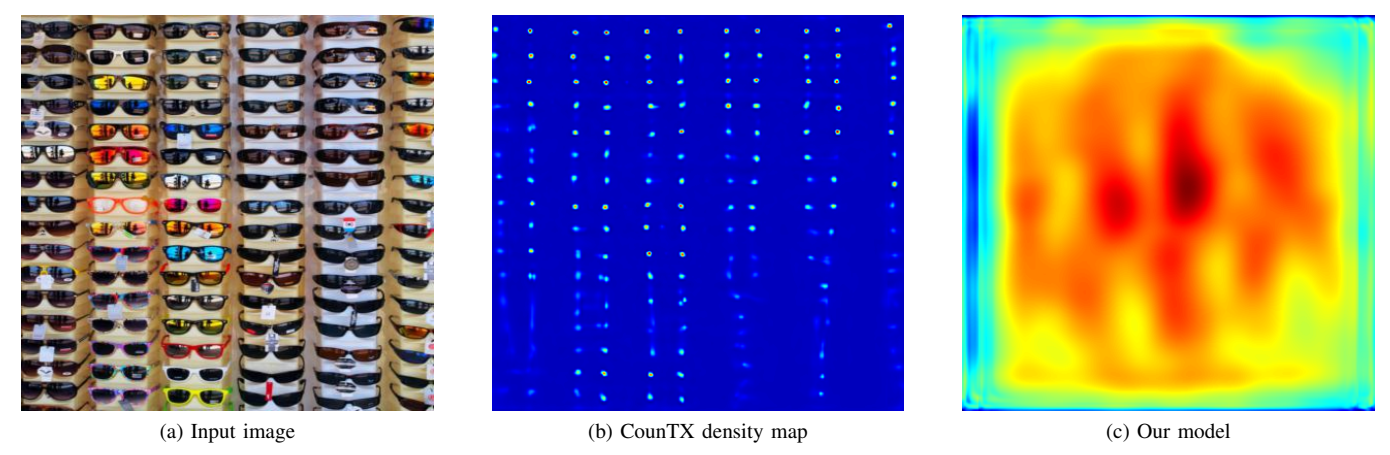


Fig. 5. Comparison on the "glasses" example from FSC-147. Ground truth (GT) count = 96; CounTX prediction = 185; our model's prediction = 98. Left to right: input image, CounTX density map, and our model's density map.

3) Decoder: The spatial feature representation, which is the output after adding visual encoder features with positional embeddings are subsequently transformed into 2D feature maps, matching the input image's original resolution. We then utilize a progressive up-sampling design, where the vector sequence is reconfigured into a dense feature map before being refined by a decoder based on ConvNet, denoted as $\mathcal{D}_{\text{Decoder}}$. This process can be represented as the following.

$$y_i = \mathcal{D}_{\mathtt{Decoder}}(\mathcal{F}_{\mathtt{E}}) \in \mathbb{R}^{H \times W \times 1}$$
 (10)

Our ConvNet consists of four up-sampling stages, each comprising a convolutional layer followed by a bilinear interpolation. Concluding this sequence of up-sampling, we employ a linear layer to serve as the density regressor, which yields a single-channel heatmap y_i indicative of object density.

C. Implementation Details

The input images are resized to a dimension of 256 x 256 pixels. Prior to model input, the images are transformed using center-cropping (224 x 224 pixels), horizontal and vertical flips, random rotations within 30 degrees, and finally, normalization. We employ the AdamW optimization method with a batch size set of 8 and a learning rate of 6.25e-6. We train our model with the RTX 3070 Ti Mobile GPU. After training for 200 epochs, the model exhibiting the lowest MAE on the validation set is chosen.

During inference time, we follow the same procedure as in [4]. Specifically, a square sliding window is adopted to scan over the image, using a stride of 128 pixels. Similar to the training phase, each image is resized to 256 x 256 pixels and subsequently normalized prior to being input into the model. For handling overlapping regions in the density map, we apply the approach described in [4].

IV. RESULTS AND DISCUSSION

A. Quantitative Results

The evaluation results for our method on FSC-147 [7] are compared against other existing methods in Table I. While not

outperforming methods like CounTR [4] and RCC [14], our model performs reasonably well across both validation and test sets. The most notable results are observed in the qualitative results in the next Section IV-B, where our model demonstrates the ability to count more complex objects that CounTR fails to.

B. Qualitative Results

Some qualitative results can be found in Figure 4, where the predicted counts from our model and from CounTX [10] have also been provided for comparison. It can be observed that the density map produced by our model is unlike the density map produced by CounTX that resembles point-level annotations.

Interestingly, the DINOv2 [6] image encoder employed in our model appears to capture structural cues that CounTX's image encoder was unable to. Revisiting the example of glasses in Figure 5, CounTX would count each lens as a single object as is evident from its resultant density map. Similarly, CounTR [4] displayed similar behaviour to CounTX and would consistently double count. As detailed in [4], test-time augmentation was required to correct the predicted count. However, our model was able to predict a similar count to

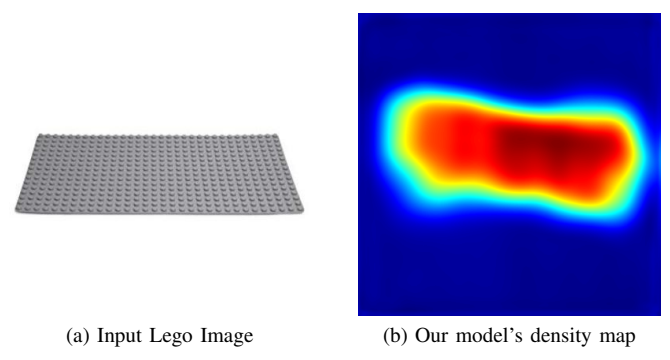


Fig. 6. Failure case on densely packed objects. Ground truth (GT) count = 512; our model's prediction = 400. Left: input image. Right: predicted density map, illustrating reduced accuracy when objects lack clear boundaries.

TABLE II PERFORMANCE OF OUR MODEL ON THE FSC-147 DATASET WITH AND WITHOUT EXCLUDED IMAGES

Configuration	Validation Set		Test Set	
	MAE	RMSE	MAE	RMSE
Without exclusions	17.66	60.77	17.49	114.99
Excluding 4 images	15.64	48.12	13.14	33.05

the ground truth without any such augmentation, possibly due to the encoder being able to encapsulate the structure of glasses within the image features and detect repetitions of this structure that corresponded to multiple glasses.

C. Exploration of Model Limitations and Future Work

Our model performs admirably across a wide variety of scenes, yet one category reveals a distinct blind-spot: the "lego pieces" scenario, where countless nearly identical small objects are tightly clustered together (see Figure 6). In those images the individual items nearly dissolve into one another — boundaries blur, repetitions overwhelm structure, and our model simply struggles. It is not a slight performance drop, it's an entire domain outside the model's strength.

While our approach handles well the majority of object classes it sees — where objects are reasonably separated, structured, and recognizable — it falters in the extreme case of densely packed, uniform objects with little visual separation. The handful of images where our model under-performs (shown in Figure 3) all share this key characteristic: minimal distinguishing features, very high repetition, and negligible spacing between instances. So, we believe there is a promising opportunity: if we were able to use higher-resolution images of the lego-piece scenes, the model's accuracy could improve significantly. The finer detail might allow the network to detect subtle boundaries, surface texture variations or structural cues that current resolution flattens out. The model works well for the vast majority of classes we evaluated, but hits a wall when faced with extreme repetition and undifferentiated visual clusters. Recognising this boundary is important — it highlights both where we succeed and where future work must go.

V. CONCLUSION

In this work, we trained a generalised visual object counter that performs without given exemplars. Taking inspiration from the CounTR [4] architecture and building upon CounTX [10], we proposed a separate visual encoder using the self-supervised model, DINOv2 [6], to obtain more informative features. The feature vectors were decoded using a ConvNet-based decoder to a density map, which was integrated to produce a predicted object count. To evaluate our model against existing methods, we used the standard counting dataset, FSC-147, and showed that our model achieves comparable results to other zero-shot methods. Most notably, the model was found to be more effective than CounTR at detecting and counting more structurally complex objects.

REFERENCES

- [1] Y. Zhang, D. Zhou, S. Chen, S. Gao, and Y. Ma, "Single-image crowd counting via multi-column convolutional neural network," in *Proceedings of the IEEE Conference on Computer Vision and Pattern Recognition (CVPR)*, June 2016.
- [2] T. N. Mundhenk, G. Konjevod, W. A. Sakla, and K. Boakye, "A large contextual dataset for classification, detection and counting of cars with deep learning," in *Computer Vision–ECCV 2016: 14th European Conference, Amsterdam, The Netherlands, October 11-14, 2016, Proceedings, Part III 14.* Springer, 2016, pp. 785–800.
- [3] E. Lu, W. Xie, and A. Zisserman, "Class-agnostic counting," in Computer Vision–ACCV 2018: 14th Asian Conference on Computer Vision, Perth, Australia, December 2–6, 2018, Revised Selected Papers, Part III 14. Springer, 2019, pp. 669–684.
- [4] C. Liu, Y. Zhong, A. Zisserman, and W. Xie, "Countr: Transformer-based generalised visual counting," arXiv preprint arXiv:2208.13721, 2022
- [5] R. Jiang, L. Liu, and C. Chen, "Clip-count: Towards text-guided zeroshot object counting," arXiv preprint arXiv:2305.07304, 2023.
- [6] M. Oquab, T. Darcet, T. Moutakanni, H. Vo, M. Szafraniec, V. Khalidov, P. Fernandez, D. Haziza, F. Massa, A. El-Nouby et al., "Dinov2: Learning robust visual features without supervision," arXiv preprint arXiv:2304.07193, 2023.
- [7] V. Ranjan, U. Sharma, T. Nguyen, and M. Hoai, "Learning to count everything," in *Proceedings of the IEEE/CVF Conference on Computer Vision and Pattern Recognition*, 2021, pp. 3394–3403.
- [8] J. Xu, H. Le, V. Nguyen, V. Ranjan, and D. Samaras, "Zero-shot object counting," in *Proceedings of the IEEE/CVF Conference on Computer* Vision and Pattern Recognition, 2023, pp. 15548–15557.
- [9] V. Ranjan and M. H. Nguyen, "Exemplar free class agnostic counting," in *Proceedings of the Asian Conference on Computer Vision*, 2022, pp. 3121–3137.
- [10] N. Amini-Naieni, K. Amini-Naieni, T. Han, and A. Zisserman, "Openworld text-specified object counting," 2023.
- [11] A. Radford, J. W. Kim, C. Hallacy, A. Ramesh, G. Goh, S. Agarwal, G. Sastry, A. Askell, P. Mishkin, J. Clark et al., "Learning transferable visual models from natural language supervision," in *International conference on machine learning*. PMLR, 2021, pp. 8748–8763.
- [12] R. Paiss, H. Chefer, and L. Wolf, "No token left behind: Explainability-aided image classification and generation," in *European Conference on Computer Vision*. Springer, 2022, pp. 334–350.
- [13] R. Paiss, A. Ephrat, O. Tov, S. Zada, I. Mosseri, M. Irani, and T. Dekel, "Teaching clip to count to ten," arXiv preprint arXiv:2302.12066, 2023.
- [14] M. Hobley and V. Prisacariu, "Learning to count anything: Referenceless class-agnostic counting with weak supervision," arXiv preprint arXiv:2205.10203, 2022.
- [15] G. Hinton, O. Vinyals, and J. Dean, "Distilling the knowledge in a neural network," 2015.
- [16] M. Caron, H. Touvron, I. Misra, H. Jégou, J. Mairal, P. Bojanowski, and A. Joulin, "Emerging properties in self-supervised vision transformers," in *Proceedings of the IEEE/CVF international conference on computer vision*, 2021, pp. 9650–9660.